Exogenous remodeling of lung resident macrophages protects against infectious consequences of bone marrow-suppressive chemotherapy

Akinobu Kamei[a,b,1], Geli Gao[a], Geoffrey Neale[c], Lip Nam Loh[a], Peter Vogel[d], Paul G. Thomas[e], Elaine I. Tuomanen[a], and Peter J. Murray[a,e,1]

[a]Department of Infectious Diseases, St. Jude Children's Research Hospital, Memphis, TN 38105; [b]Department of Pediatrics, Keio University School of Medicine, Tokyo 160-8582, Japan; [c]Hartwell Center for Bioinformatics and Biotechnology, St. Jude Children's Research Hospital, Memphis, TN 38105; [d]Department of Pathology, St. Jude Children's Research Hospital, Memphis, TN 38105; and [e]Department of Immunology, St. Jude Children's Research Hospital, Memphis, TN 38105

Edited by Ruslan Medzhitov, Yale University School of Medicine, New Haven, CT, and approved August 9, 2016 (received for review May 15, 2016)

Infection is the single greatest threat to survival during cancer chemotherapy because of depletion of bone marrow-derived immune cells. Phagocytes, especially neutrophils, are key effectors in immunity to extracellular pathogens, which has limited the development of new approaches to protect patients with cancer and chemotherapy-induced neutropenia. Using a model of vaccine-induced protection against lethal *Pseudomonas aeruginosa* pneumonia in the setting of chemotherapy-induced neutropenia, we found a population of resident lung macrophages in the immunized lung that mediated protection in the absence of neutrophils, bone marrow-derived monocytes, or antibodies. These vaccine-induced macrophages (ViMs) expanded after immunization, locally proliferated, and were closely related to alveolar macrophages (AMs) by surface phenotype and gene expression profiles. By contrast to AMs, numbers of ViMs were stable through chemotherapy, showed enhanced phagocytic activity, and prolonged survival of neutropenic mice from lethal *P. aeruginosa* pneumonia upon intratracheal adoptive transfer. Thus, induction of ViMs by tissue macrophage remodeling may become a framework for new strategies to activate immune-mediated reserves against infection in immunocompromised hosts.

chemotherapy | neutropenia | vaccine | macrophage | *Pseudomonas aeruginosa* pneumonia

Chemotherapy and radiotherapy have been mainstays of cancer treatment for ∼80 y (1). Both therapies target dividing cells with the collateral cost of damaging and killing proliferating noncancerous cells in essential tissues such as bone marrow, lung, gut, skin, and mucosal surfaces. Defining the resources the body could use to adapt to broad tissue damage is essential to mitigating the negative effects of current cancer therapy.

Humans make $\sim 10^9$ neutrophils per kilogram per day, a rate that increases after infection by bacteria, fungi, viruses, and parasites (2). Chemotherapy agents such as cyclophosphamide (CY) kill dividing cells in the granulocyte–macrophage progenitor fraction of the bone marrow. Neutropenia ($<0.5 \times 10^3$ neutrophils per microliter of blood) is a prevalent consequence of chemotherapy-induced damage to the bone marrow, and the degree of neutropenia correlates with the incidence of life-threatening infections (3–5). Neutropenia can be abated in some cases by systemic granulocyte colony-stimulating factor (G-CSF) therapy that forces the remnant neutrophil progenitors into cycle (6). However, when the progenitors are severely depleted or damaged by intense chemotherapy, G-CSF cannot induce neutrophil rebound and the patient remains at risk for serious infections.

Here, we determined that the lung immune microenvironment harbors myeloid cells that can expand by exogenous stimulation, survive chemotherapy, and mediate host defense against lethal bacterial infection in the setting of chemotherapy-induced bone marrow suppression. Our whole-animal model sequentially combined three components: vaccination with a live-attenuated *Pseudomonas aeruginosa* vaccine; CY as the systemic bone marrow-suppressive chemotherapy agent; and challenge with virulent *P. aeruginosa*, the leading cause of bacterial pneumonia in patients with cancer and neutropenia (7). We found that resident lung macrophages, most of which originate in embryogenesis, respond to vaccination and protect the lung in the absence of circulating neutrophils, antibodies, or bone marrow-derived monocytes normally required for lung protection in infection. Our study suggests ways to harness the natural defensive capacity of lung resident macrophages to compensate for depletion of neutrophils in cancer therapy.

Results

Vaccination Protects Against Lethal *P. aeruginosa* Pneumonia During Chemotherapy. Neutrophils are essential for immunity to *P. aeruginosa* (8, 9), the leading cause of bacterial pneumonia in patients with cancer and neutropenia (7). First, we validated our animal model of lethal *P. aeruginosa* pneumonia in the setting of chemotherapy-induced neutropenia. CY treatment alone without bacterial challenge did not cause death (Fig. 1*A*). Mice that were not treated with CY survived intranasal (i.n.) infection with *P. aeruginosa* strain IT4 (10) at 7.7×10^5 cfu. In contrast, when mice were pretreated with CY, a challenge dose of 77 cfu (10^4-fold less than the dose used for CY-untreated mice) led to 100% mortality

Significance

Infectious complications can be lethal in patients with cancer when chemotherapy depletes white blood cells (WBCs) needed to clear microbes. Prevention of infection by vaccination also requires WBCs, and thus has not been effective in saving patients with low WBC counts during chemotherapy. Using a mouse model, we discovered a kind of lung WBC that survives chemotherapy. This cell is found in the lung and can engulf and remove bacteria when activated by a vaccine. This vaccination strategy results in excellent survival in a mouse model of lethal bacterial pneumonia in the setting of chemotherapy. These findings suggest that a protective, chemotherapy-stable lung WBC could be exogenously induced to protect patients with cancer who are at high risk of life-threatening infections.

Author contributions: A.K., P.G.T., E.I.T., and P.J.M. designed research; A.K., G.G., and L.N.L. performed research; P.J.M. contributed new reagents/analytic tools; A.K., G.N., L.N.L., P.V., P.G.T., E.I.T., and P.J.M. analyzed data; and A.K., E.I.T., and P.J.M. wrote the paper.

The authors declare no conflict of interest.

This article is a PNAS Direct Submission.

Data deposition: The data reported in this paper have been deposited in the Gene Expression Omnibus (GEO) database, www.ncbi.nlm.nih.gov/geo (accession no. GSE85336).

[1]To whom correspondence may be addressed. Email: peter.murray@stjude.org or akinobu.kamei@stjude.org.

This article contains supporting information online at www.pnas.org/lookup/suppl/doi:10.1073/pnas.1607787113/-/DCSupplemental.

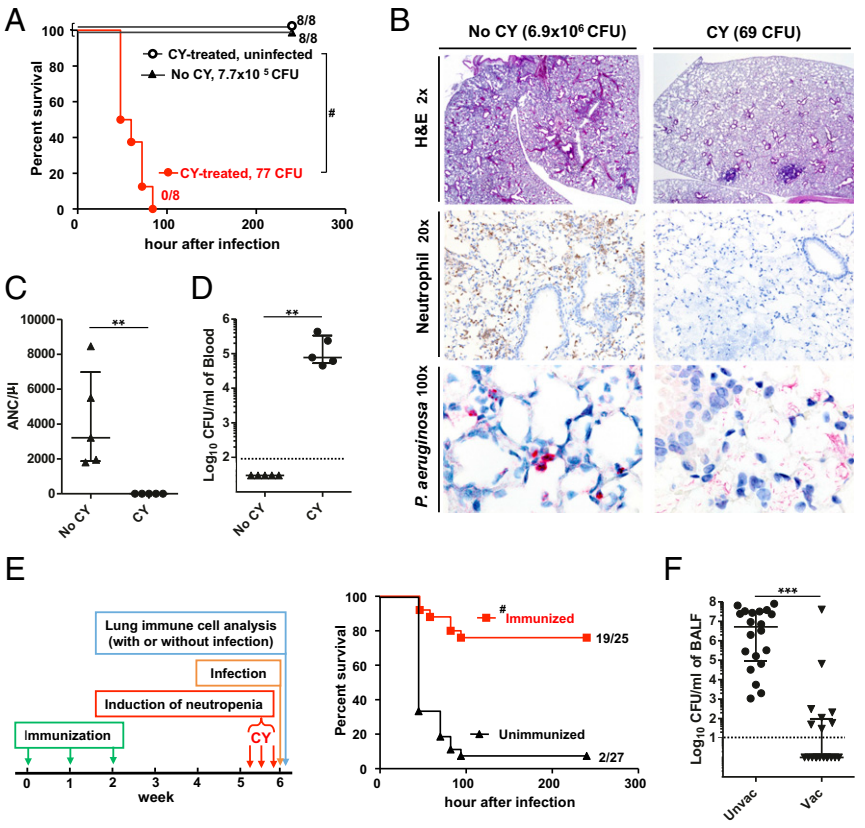

Fig. 1. Mouse model of immunization and lethal *P. aeruginosa* pneumonia during chemotherapy-induced neutropenia. (*A*) Survival of mice ± CY treatment (no. alive/total as indicated) at the challenge doses shown. (*B*) Representative photomicrographs of lung histology (*Top*; H&E stain) and immunohistochemistry (IHC) stain for neutrophils (*Middle*) and *P. aeruginosa* (*Bottom*). Blood neutrophil counts (*C*) and blood *P. aeruginosa* burden (*D*) from mice ± CY 30 h after challenge ($n = 5$ per group; challenge dose of 6.9×10^6 cfu for No CY or 69 cfu for CY). (*E*) Time line of the standard experimental treatment schedule (*Left*) and survival of immunized or unimmunized mice after challenge following CY treatment (*Right*, no. alive/total as indicated). Data combined from two independent experiments (challenge doses of 52–61 cfu) are shown. (*F*) *P. aeruginosa* burden in BALF 30 h postchallenge in CY-treated mice ± prior vaccination ($n = 20$ per group). Data combined from two independent experiments (challenge doses of 68–70 cfu) are shown. Each symbol in the graphs represents one mouse, and error bars represent median with interquartile ranges. Dashed lines represent lower limit of detection. $^{**}P < 0.01$ and $^{***}P < 0.001$ by the Mann–Whitney test; $^{\#}P < 0.0001$ by log-rank test.

(Fig. 1*A*). Lung histopathology 30 h after challenge demonstrated neutrophil infiltration in the lung of CY-untreated mice (Fig. 1*B*, *Left*), which was associated with elevated blood neutrophil numbers (Fig. 1*C*) and without secondary bacteremia (Fig. 1*D*). In CY-treated mice, neutrophils were absent in the lung tissue where the bacteria were abundant (Fig. 1*B*, *Right*), which was associated with neutropenia (Fig. 1*C*) and high-grade bacteremia (Fig. 1*D*). Thus, in the setting of CY-induced neutropenia, even a low dose of *P. aeruginosa* expanded in the lung and spread systemically, leading to death.

To test the idea that a neutropenic host could be protected against lethal *P. aeruginosa* infection by vaccination, mice were i.n. immunized with three weekly doses of live-attenuated *P. aeruginosa* vaccine strain PAO1Δ*aroA* (11) and then challenged 4 wk later i.n. with wild-type *P. aeruginosa* strain IT4 (a strain bearing heterologous lipopolysaccharide O-antigens compared with the vaccine stain) following three doses of CY (Fig. 1*E*, *Left*). Immunized mice were protected from the lethal infection in the context of CY treatment (Fig. 1*E*, *Right*). This vaccine-induced protection was associated with an ~5-$\log_{10}$ reduction in bacterial load in the lungs (Fig. 1*F*). Thus, vaccination was protective, even in the absence of neutrophils.

Lung Macrophages Are Required for the Vaccine-Induced Protection During Neutropenia. The data in Fig. 1 suggested that vaccination altered the lung immune microenvironment to compensate for the absence of neutrophils. Because phagocytes are the primary terminal effectors in clearance of extracellular bacteria, we quantified the number and proportions of phagocytes in the lung during infection in CY-untreated normal mice (controls) and CY-treated mice with or without preceding vaccination (gating strategy in Fig. S1). In CY-treated mice, all of the phagocytes except for F4/80$^+$ macrophages were depleted from the bronchoalveolar lavage fluid (BALF) regardless of the vaccination history (Fig. 2 *A* and *B*). Importantly, prior vaccination was associated with higher numbers of F4/80$^+$ macrophages in the BALF during infection (Fig. 2*B*). Neutrophil depletion and persistence of F4/80$^+$ cells after CY treatment were also confirmed in the lung parenchyma of immunized mice (Fig. 2*C*). Thus, macrophages are the primary remnant phagocytes in the lung associated with vaccine-induced protection in the setting of chemotherapy-induced neutropenia.

Bacterial clearance by phagocytes is enhanced by humoral and cellular immune effectors induced by the *P. aeruginosa* live-attenuated vaccines such as antibodies and Th17 cells (12, 13). To determine if adaptive effectors also contribute to protection in the current model, we tested for the vaccine efficacy in B-cell–deficient (μMT) mice and *Rag2*$^{-/-}$ mice. B-cell–deficient mice were protected by the vaccination (Fig. S2*A*), confirming that antibodies are not required for the protection. In contrast, vaccine efficacy was abolished in *Rag2*$^{-/-}$ mice (Fig. S2*B*), suggesting critical contributions by T cells in bacterial clearance by

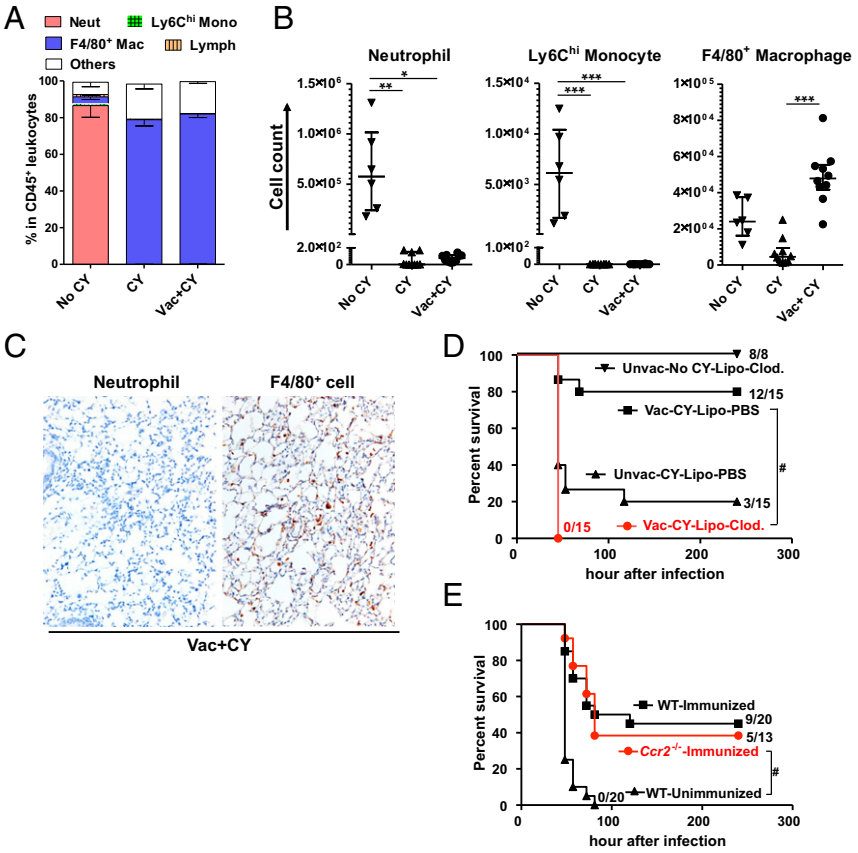

Fig. 2. Macrophages are required for vaccine-induced protection during chemotherapy. Quantitation of immune cell types in BALF during infection expressed as the fraction in total $CD45^+$ leukocytes recovered from the total BALF per mouse (*A*) or by absolute number in the BALF (*B*). Mono, monocyte; Neut, neutrophil; Vac, PAO1Δ*aroA*-immunized; Vac+CY, immunized plus CY-treated. BALF was obtained from untreated mice or CY-treated mice ± prior vaccination 30 h after *P. aeruginosa* challenge ($n = 6$–10 per group; 6.8×10^6 cfu for untreated mice and 68 cfu for CY-treated mice). Each symbol represents one mouse, and error bars represent median with interquartile ranges. $^*P < 0.05$, $^{**}P < 0.01$, and $^{***}P < 0.001$ by the Kruskal–Wallis test, followed by Dunn's multiple comparisons test. (*C*) IHC stain for neutrophils (negative) or $F4/80^+$ cells (brown) in lung parenchyma of immunized, CY-treated mice 30 h post-infection (69 cfu). A positive neutrophil stain performed side by side with these samples is shown in Fig. 1*B*. Representative data are shown from five mice. (Magnification: 20×). (*D*) Survival of immunized, CY-treated mice given either i.n. liposomal clodronate (lipo-Clod.) or lipo-PBS 24 h before challenge (65 cfu; no. alive/total as indicated). Unimmunized, CY-treated mice with i.n. lipo-PBS before challenge (65 cfu) or unimmunized, CY-untreated normal mice with i.n. lipo-Clod. before challenge (5.8×10^5 cfu, performed in an independent experiment from the other groups) were controls. Survival was monitored twice daily starting 24 h postinfection. $^{\#}P < 0.0001$ by log-rank test. Unvac, unvaccinated. (*E*) Survival of CCR2-deficient mice that were immunized, CY-treated, and challenged (60–69 cfu; no. alive/total as indicated). Immunized or unimmunized wild-type mice that were challenged following CY treatment were controls. Data combined from two independent experiments are shown. $^{\#}P < 0.0001$ by log-rank test.

the remnant phagocytes in the lung. Although numbers of lung $CD4^+$ and $CD8^+$ cells declined ∼10-fold following CY treatment (Fig. S2*C*), our data suggest certain remnant T-cell populations, such as pulmonary resident memory T cells, are likely to play some roles in phagocyte-mediated bacterial clearance.

Next, to confirm whether macrophages were the critical effector of the vaccine efficacy during chemotherapy-induced neutropenia, we performed in vivo macrophage depletion experiments. In the absence of CY treatment, i.n. administration of liposomal clodronate before *P. aeruginosa* challenge (strain IT4, 5.8×10^5 cfu) did not affect the survival of mice (Fig. 2*D*), where ∼90% of $F4/80^+$ macrophages were depleted from the BALF, but in the presence of neutrophil accumulation during infection (Fig. S3*A*). In the setting of CY-induced neutropenia, however, an $\sim\log_{10}$ reduction of $F4/80^+$ by i.n. liposomal clodronate (Fig. S3*B*) abolished the vaccine efficacy (Fig. 2*D*), confirming that lung macrophages that survive CY treatment are required for the vaccine-induced protection in the setting of neutropenia.

In addition to disrupting neutrophil production, systemic chemotherapy targets monocytes, which originate from the same myeloid progenitor pools as neutrophils and seed the macrophage lung pool. Bone marrow-derived inflammatory monocytes recruited from the blood following signals from the chemokine (C-C motif) ligand 2 (CCL2) are essential for controlling lung infections (14–17). Although CY significantly depleted Ly-$6C^{hi}$ monocytes from the whole lung (Fig. S4), the possibility remained that residual bone marrow-derived monocytes could contribute to the protective effects of vaccination. To distinguish between the contributions of local lung macrophages versus bone marrow-derived macrophages, we immunized chemokine (C-C motif) receptor 2 (CCR2)-deficient mice and challenged with the bacteria after CY treatment. Survival curves were identical between the vaccinated wild-type mice and vaccinated $Ccr2^{-/-}$ mice (Fig. 2*E*). We therefore concluded a CCR2-independent macrophage population contributed to protective lung immunity in chemotherapy-induced neutropenia.

Lung resident macrophages comprise two ontologically distinct groups: alveolar macrophages (AMs) and interstitial macrophages (IMs). AMs originate in the embryo and are self-maintained in adults with very slow turnover at homeostasis (18–20). They patrol air-exposed surfaces of alveoli, are dependent on granulocyte-macrophage (GM)-CSF, and can divide to replace cells lost during

infection or damage (21). IMs populate the interstitial spaces between alveoli and are derived from the bone marrow (22). Extensive ontogenic studies and phenotyping of the different myeloid cells have allowed unambiguous discrimination of the different lung myeloid populations (18, 22–27). To identify the lung resident macrophages associated with protection, we undertook a phenotypic analysis of the lung macrophage populations in vaccinated or unvaccinated mice with or without CY treatment. Of note, the analysis was performed in the absence of bacterial challenge to elucidate the baseline lung macrophage subsets in chemotherapy-treated hosts when they first encounter microorganisms. Building upon flow cytometric studies of lung myeloid cells (18, 21–23, 25–27), we adopted a gating scheme that reproducibly identified macrophages in vaccinated, CY-treated lungs (Fig. 3*A*). CY treatment caused elimination of Ly6G$^+$ cells (neutrophils) as expected. Within the CD45$^+$ Lin$^-$ fraction, CD11b was used to identify CD11b^{lo} and CD11b^{hi} fractions that were subfractionated with CD11c and MHCII. Using this approach, the CD11b^{lo}, CD11c^{hi}, MHCII^{lo} cells were designated as AMs (population "C" in Fig. 3*A*), which was confirmed by an alternate strategy and additional surface markers (22, 25, 28, 29) (Fig. S5 *A* and *B*).

The CD11b^{hi} fraction contained multiple populations that were separated with CD11c and MHCII staining. The CD11b^{hi}, CD11c^{lo}, MHCII^{hi} cells (population "B" in Fig. 3*A*) were designated IMs, as confirmed by an alternate gating strategy and additional surface markers (22, 25, 28, 29) (Fig. S5 *A* and *B*), although we note this population B potentially incudes lung dendritic cell (DC) subsets. Vaccination, with or without CY treatment, resulted in the appearance within the CD11b^{hi} fraction of CD11c^{hi}, MHCII^{lo} cells (population "A" in Fig. 3*A*). For brevity, we termed these cells

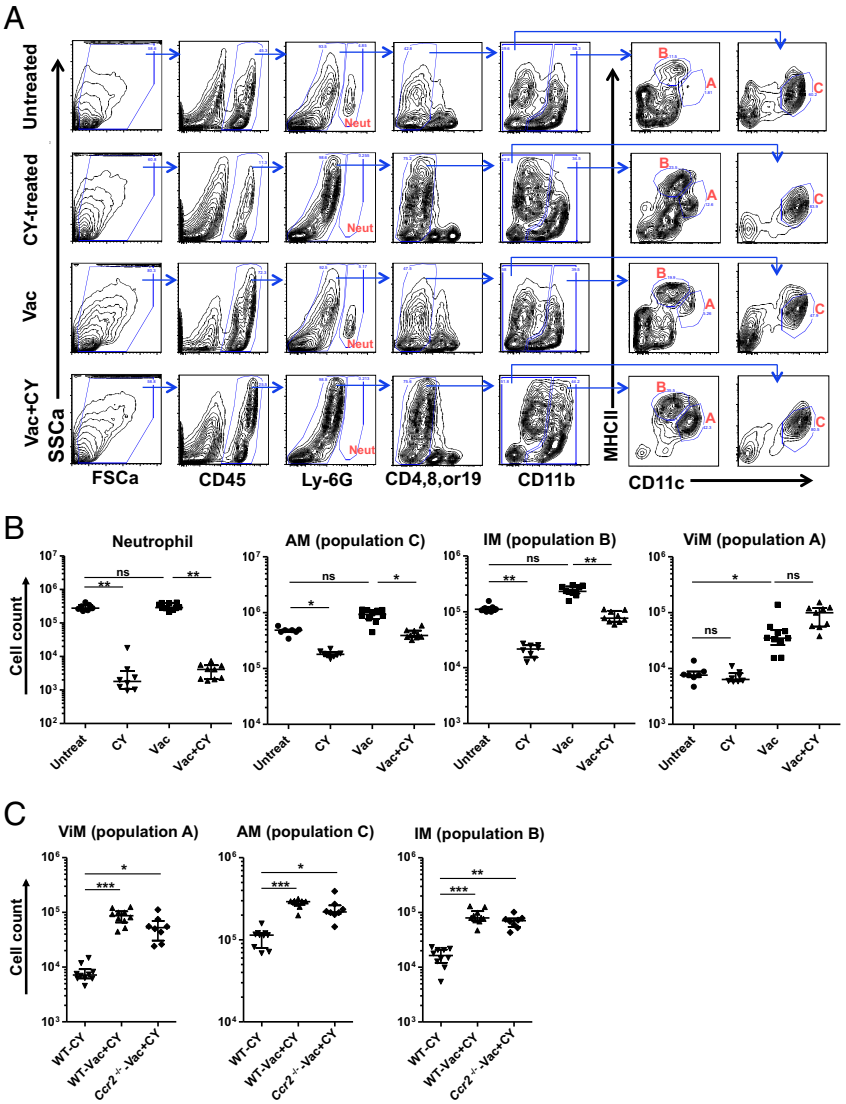

Fig. 3. Alterations in lung myeloid cell composition induced by immunization and chemotherapy. (*A*) Representative flow data from collagenase-digested whole-lung samples from untreated, CY-treated, Vac, or Vac+CY mice. Note the three dominant cell populations (populations A, B and C in red) in the lungs from Vac+CY mice. FSCa, forward scatter; SSCa, side scatter. (*B*) Cell numbers for neutrophils, AMs (population C), IMs (population B), and ViMs (population A) in the lungs from mice treated as indicated (n = 7–10 per group). (*C*) Macrophage counts in the lungs from wild-type (WT) or CCR2-deficient mice that were immunized and CY-treated. Unimmunized WT mice treated with CY were controls (n = 8–10 per group). Each symbol in the graphs represents one mouse, and error bars represent median with interquartile ranges. *P < 0.05, **P < 0.01, and ***P < 0.001 by the Kruskal–Wallis test, followed by Dunn's multiple comparisons test (comparisons were made between untreated (Untreat) vs. Vac, Untreat vs. CY, and Vac vs. Vac+CY in *B*). ns, not significant. Lungs were harvested at 4 wk after the third dose of vaccination and 2 d after the third dose of CY. Data are representative of at least two independent experiments.

"vaccine-induced macrophages" (ViMs). The current gating strategy (Fig. 3*A*) uses MHCII expression levels to exclude lung DCs from populations A and C, whereas the alternate strategy (Fig. S5*A*) uses MerTK and CD64 expression to exclude lung DC subsets robustly (29). To rule out the possibility of substantial DC contaminations into population A, B, or C (Fig. 3*A*) in vaccinated plus CY-treated mice, we compared the fractions of AMs, IMs, or ViMs within total lung leukocytes measured by those two gating schemes using the same samples, and the numbers were not significantly different (Fig. S5*C*).

ViMs Expand by Vaccination and Are Stable in Number Through Chemotherapy. Next, we performed a quantitative analysis of ViMs following vaccination. Over the three weekly doses of immunization, ViMs expanded in absolute number as well as in relative proportion within total lung leukocytes when measured at 1 wk after each vaccine dose (Fig. S6*A*). We next quantified the number of ViMs and the other phagocytes in the lung with or without CY treatment at 4 wk after the third dose of vaccination, at which time point mice were challenged for survival studies. In both vaccinated and unvaccinated mice, when neutrophil numbers precipitously declined after CY treatment (Fig. 3*B*), the absolute number of AMs (population C) and IMs (population B) also declined following chemotherapy (Fig. 3*B*). In contrast, ViMs (population A) showed no significant change in absolute number after CY treatment (Fig. 3*B*) (with a trend for increase in number following CY but only in vaccinated mice) and demonstrated an ~$\log_{10}$ increase when expressed as a relative proportion in the total lung leukocytes (Fig. S6*B*). These data were further confirmed by measuring the lung cell counts for ViMs, AMs, IMs, and neutrophils after no, one, two, or three doses of CY. Under these conditions, only ViMs were stable in number, whereas the others declined over the dosing regime (Fig. S6*C*). Furthermore, for each of these macrophage populations, the lung cell counts in vaccinated, CY-treated mice were comparable between wild-type mice and *Ccr2*$^{-/-}$ mice (Fig. 3*C*). Therefore, expansion of the ViMs (CD11b^{hi}, CD11c^{hi}, MHCII^{lo}) by vaccination and persistence during chemotherapy occurred in mice bearing genetic depletion of circulating bone marrow-derived monocytes.

Lung CD11b^{hi}, CD11c^{hi}, MHCII^{lo} Macrophages Are Related to AMs. We next sought to determine the relationship of ViMs to other resident lung macrophage populations. AMs populate the air-exposed surfaces of the alveolar sacs and are present in lung lavage fluid, whereas IMs reside in the lung interstitium providing a means to distinguish the anatomical location of the ViMs compared with IMs that are recovered only from whole-lung digests. Comparison of immune cell counts in BALF versus postlavage whole lung from immunized, CY-treated mice revealed that the recovery rate of ViMs by BAL was equivalent to the recovery rate of AMs and ~20-fold higher than IMs (Fig. 4*A*), suggesting that ViMs were associated with the air interface of the alveolar sacs at steady state. ViMs were autofluorescent in the FITC channel, sialic acid-binding Ig-like lectin-F^{+} (Siglec-F^{+}), and F4/80^{+}, features characteristic of AMs (29) (Fig. 4*B*). However, observation of the cytocentrifuged macrophages revealed that although AMs had morphology consistent with prior reports, where the cells are round in shape with a large round nucleus (23, 26, 27), ViMs were smaller in size with irregular nuclear morphology (Fig. 4*C*). These data prompted us to take a molecular approach to analyze ViMs further. Recent parabiosis data and advanced flow cytometry approaches have identified markers that distinguish between embryonic-derived AMs and blood-derived macrophages (e.g., IMs) at homeostasis (22).

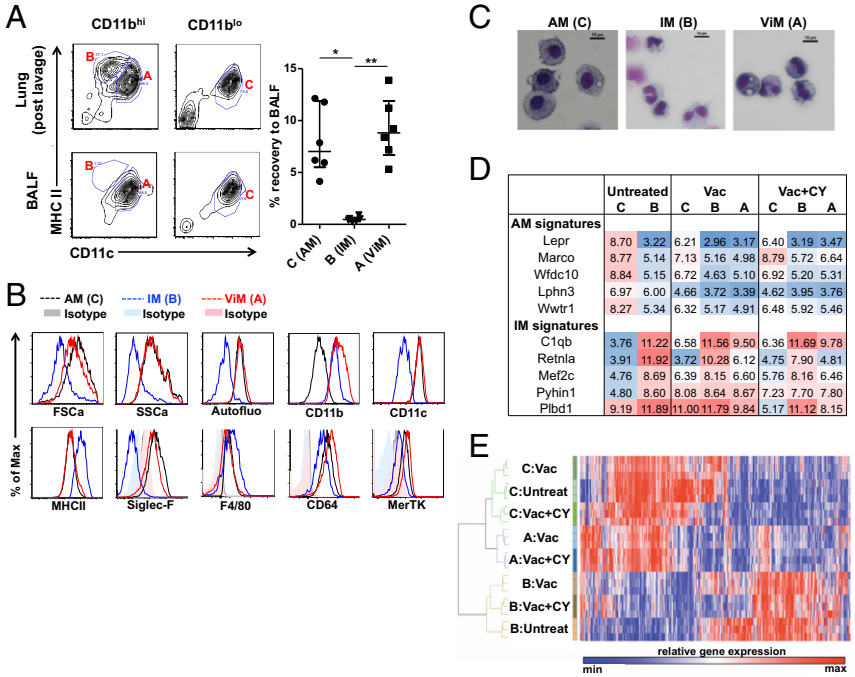

Fig. 4. Characterization of lung macrophages in the context of immunization and CY treatment. (*A*) Representative flow data on BALF (*Left Lower*) or postlavage whole-lung samples (*Left Upper*) from immunized plus CY-treated mice. (*Right*) Fraction of the cells recovered from the lungs by bronchoalveolar lavage is shown. Each symbol represents one mouse, and error bars represent median with interquartile ranges. *$P < 0.05$ and **$P < 0.01$ by the Kruskal–Wallis test, followed by Dunn's multiple comparisons test. (*B*) Flow cytometric analysis of each macrophage population. Max, maximum. (*C*) Gross morphology of cytocentrifuged macrophages with Giemsa stain. (Scale bars: 10 μm.) (*D*) Tabulation of relative gene expression ($\log_2$[Signal]) associated with homeostatic populations of AMs or IMs as assigned by Gibbings et al. (22). C, B, and A refer to the lung macrophage populations defined in C. (*E*) Hierarchical clustering of lung macrophages from mice treated as indicated. Shown is a heat map and clustering based on 4,984 robustly expressed RNA transcripts (greater than twofold over background) with greater than twofold differential expression across cell populations.

For example, leptin receptor is very highly expressed in AMs relative to all other myeloid cells, and is stably expressed across time of residence in the lung. We investigated the mRNA expression of five markers of AMs (Lepr, Marco, Wfdc10, Lphn3, and Wwtr1) or IMs (C1qb, Retnla, Mefc2, Pyhin1, and Plbd1) in each lung macrophage population. Of note, ViMs are not substantially present in unimmunized normal mice (Fig. 3*B*). As shown in Fig. 4*D*, the patterns of expression of the 10 mRNAs showed the expected differences between AMs and IMs from untreated mice. In vaccinated mice with or without CY, the same markers showed new patterns for AMs and ViMs, but not for IMs, suggesting modulation by mucosal immunization 4 wk prior or cytotoxic chemotherapy for AMs and ViMs.

We next isolated AMs and the two CD11b^{hi} macrophage populations from untreated mice; immunized mice; or immunized, CY-treated mice and compared their global transcriptomes. Using the Pearson correlation, we found the ViMs were closely related to AMs but distinct from IMs at the transcriptome level (Fig. 4*E*). Of note, ViM gene expression profiles were not concordant with the signature of epidermal Langerhans cells that are resistant to ionizing irradiation (30) (Fig. S7). Taken together, cellular and molecular evidence indicates that ViMs, the chemotherapy-stable lung resident macrophages that expand by vaccination, are related to AMs. Because CD11b is modulated by activation on AMs (23, 24), our data are consistent with a model where ViMs are an activated form of resident AMs.

Physiological Characteristics of ViM. AMs derive from embryonic monocytes that seed the lung and are maintained locally after birth under homeostatic conditions where their replacement with bone marrow-derived macrophages occurs very slowly over years (18, 20, 21, 31). To ensure adequate AM number as the lung grows in size or repairs after damage, AMs have GM-CSF–dependent proliferative capacity (21). Given that ViMs have characteristics of activated AMs, we determined if these macrophages had proliferative capacity. Untreated mice or mice immunized 4 wk prior with or without subsequent CY were treated with BrdU for 3 d, followed by measurement of BrdU incorporation into AMs or ViMs. Without CY, ~10% or more of the cells were BrdU^{+} in both macrophage populations (Fig. 5*A*), indicating those macrophages or their progenitors had undergone cell division in the preceding 72 h. These data were further confirmed with Ki-67 expression by

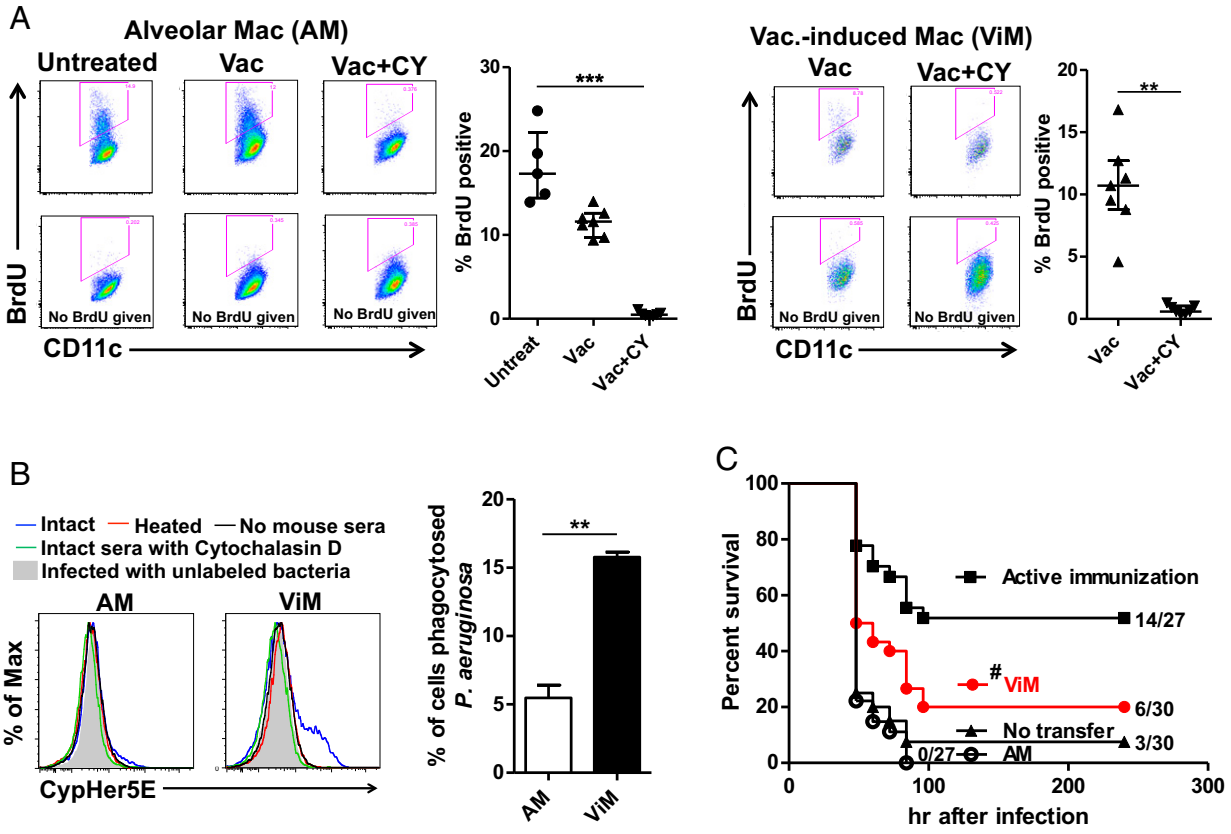

Fig. 5. ViMs are protective against bacterial infection in neutropenic hosts. (*A*) BrdU incorporation into lung macrophages in untreated mice or mice at 4 wk after vaccination ± CY (n = 5–7 per group). Mice were labeled i.p. with BrdU for 3 d before lung harvest. Representative flow data and BrdU^{+} fractions in macrophage (Mac) gates are shown for AMs (*Left*) and ViMs (*Right*). Data are representative of two independent experiments. Each symbol represents one mouse, and error bars represent median with interquartile ranges. ***P < 0.001 by the Kruskal–Wallis test, followed by Dunn's multiple comparisons test for AMs. **P < 0.01 by the Mann–Whitney test for ViMs. (*B*) Phagocytic activity of AMs and ViMs in vitro. Macrophages isolated from the lungs pooled from Vac+CY-treated mice (n = 17–25 animals) were incubated in vitro with CypHer5E-labeled *P. aeruginosa* strain IT4 (in vivo challenge strain, LPS O-antigens heterologous to the vaccine strain) for 60 min in the presence of either intact or heat-inactivated sera from PAO1Δ*aroA*-immunized mice. Representative flow data (*Left*) and the fluorescence-positive fractions in macrophage gates in the presence of intact sera (*Right*) are shown. Bars represent mean of data from two independent experiments (three replicates for each). Error bars represent SEM. **P < 0.01 by unpaired t test. (*C*) Effect of macrophage adoptive transfer on survival (no. alive/total as indicated). AMs or ViMs isolated from the lungs pooled from immunized plus CY-treated mice were intratracheally administered (1×10^5 cells per mouse) to unimmunized CY-treated mice. Recipients were challenged 14 h after the transfer. Unimmunized mice or actively immunized mice (both treated with CY) that did not receive the macrophages were controls. Data combined from two independent experiments (challenge doses of 59–63 cfu) are shown. #P = 0.03023 by log-rank test comparing ViM transfer vs. no transfer.

the macrophages (Fig. S8), suggesting that, like AMs, ViMs locally proliferate under homeostasis. BrdU incorporation and Ki-67 expression were reduced by CY treatment (Fig. 5*A* and Fig. S8), as expected for a cytotoxic drug that targets mitotic cells.

In the absence of neutrophils, even a low dose of *P. aeruginosa* expanded in the lung and spread systemically (Fig. 1 *B*–*D*). However, in vaccinated mice, the bacterial expansion in the lung was suppressed (Fig. 1*F*), which correlated with the survival advantage (Fig. 1*E*). To account for this difference in bacterial clearance, we documented the phagocytic capacity of ViMs using fluorescent polystyrene beads or CypHer5E-labeled *P. aeruginosa* strain IT4. CypHer5E is a pH-sensitive dye that fluoresces only when bacteria are delivered to the acidic environment of phagosomes (32), thus differentiating phagocytosed bacteria from bacteria remaining outside the cell. ViMs phagocytosed both polystyrene beads and bacteria more efficiently than AMs (Fig. 5*B* and Fig. S9). In this in vitro system, the superior bacterial phagocytosis by ViMs was documented in the presence of intact immunized mouse sera, but not heat-inactivated immune sera (Fig. 5*B*), suggesting heat-liable factors, such as complement, contribute to the superior phagocytic activity of ViMs.

Based on the increased phagocytic capacity of ViMs, we next evaluated if direct transfer of purified ViMs into unvaccinated CY-treated mice could provide baseline protection against bacterial challenge. We therefore compared the protective efficacy against lethal *P. aeruginosa* pneumonia of ViMs versus AMs upon intratracheal adoptive transfer of the cells in unimmunized neutropenic mice. At an intratracheal dose of 1×10^5 cells per mouse, only ViMs prolonged the survival of the neutropenic, infected mice (Fig. 5*C*). It should be noted that this protective effect was unexpected, because macrophages transferred into the lung, regardless of their origin, rapidly (within days) alter their phenotype (33, 34). Overall, based on depletion (Fig. 2*D*), population stability (Fig. 3*B*), ex vivo phagocytosis (Fig. 5*B*), and transfer (Fig. 5*C*), we concluded ViMs are essential protective cells in the lung that adapt to the altered local and systemic immune environment caused by the chemotherapy.

Discussion

Infectious complications remain a major obstacle to the effective management of patients with cancer. We conducted this study to elucidate the immune mechanisms that are stable during chemotherapy and could compensate for chemotherapy-induced bone marrow suppression. We have discovered a previously unrecognized lung macrophage population, termed here ViM, which survives chemotherapy and mediates protection against lethal *P. aeruginosa* pneumonia when activated by vaccination. This finding suggests that immune-mediated "reserve" pathways exist for the host to survive life-threatening infections in the setting of chemotherapy-induced ablation of normal hematopoiesis. ViMs protect the lungs from lethal bacterial infection in the setting of profound neutropenia. Importantly, ViMs are active under coincident chemotherapy-induced monocytopenia, or monocytopenia caused by genetic inactivation of the CCL2/CCR2 axis. Collectively, our results argue that exogenous conditioning of the lung immune microenvironment is a potential strategy to protect the lung during chemotherapy independent of bone marrow seeding of myeloid cells to the lungs. In the current protection model, where ViMs served as the key terminal effector of bacterial clearance, antibodies were not required. In contrast, comparison of vaccine efficacy in B-cell–deficient versus T- and B-cell–deficient mice indicated that T cells were required at some point for the protection. It is possible that lung resident memory T-cell populations assisted the macrophage-mediated bacterial clearance by enhancing, for example, expansion, survival, and/or activity of ViMs. However, to elucidate the precise nature of the T-cell–ViM interplay, the use of tools to deplete or transfer specific T-cell subsets accurately will be required, and at specific times in the vaccine-chemotherapy-infection model.

ViMs are a population of $CD11c^{hi}$, $MHCII^{lo}$ macrophages within the $CD11b^{hi}$ fraction that increase with vaccination but are not depleted by CY treatment. Four lines of evidence are consistent with the concept that ViMs are closely related to AMs. First, these cells are associated with the airway lumen. Second, at the whole-transcriptome level, ViMs cluster with AMs but not IMs. Third, ViMs are autofluorescent, $F4/80^+$, and $Siglec\text{-}F^+$, hallmarks of AMs (26, 27, 29). Fourth, ViMs are observed in CCR2-deficient mice, which have reduced numbers of circulating monocytes. However, we note that ViMs lose the normal AM morphology. Furthermore, hallmark gene expression patterns of lung AMs in homeostasis, such as the leptin receptor mRNA (22), were modulated in ViMs. The simplest interpretation of the totality of the data is that ViMs are a form of activated AM that is locally maintained by proliferation and effectively protects the lung from infections in the absence of neutrophils. Whether ViMs originate from the sessile or nonsessile AMs (35) remains to be elucidated. A different interpretation of these data is that a CCR2-independent blood-derived cell could populate the lung and expand after vaccination. Given that macrophages from non-lung sources rapidly acquire characteristics of lung macrophages after transfer (33, 34), it is possible that a nonresident lung macrophage migrates to the lung and could turn into ViMs. Differentiating between the activated AM versus migratory CCR2-independent models will require use of techniques such as lineage tracing or parabiosis, but in the setting of vaccination, chemotherapy, and lung challenge as described here. Regardless of where the ViMs come from, their functional properties convey protection to the host in chemotherapy-induced neutropenia. ViMs are proliferative to a degree similar to AMs, but their numbers are more stable than AMs under chemotherapeutic duress. The mechanisms whereby ViMs show more enhanced chemotherapy stability than AMs remain unclear at present. We note that this stability was not linked solely to increased expression of cyclin-dependent kinase inhibitor p21 as was reported in radiation resistance by epidermal Langerhans cells (30).

ViMs are highly phagocytic for *P. aeruginosa*, which is likely to contribute to their ability to eradicate the bacteria efficiently at an early stage of infection. ViMs are also protective against bacterial challenge when transferred into unvaccinated neutropenic hosts. Defining the live-attenuated vaccine component that could effectively expand ViM may lead to a safer vaccine candidate for lung infections in bone marrow-suppressed patients. In addition, we suggest that CD11b could be used as a surrogate marker to identify additional human lung macrophages that are activated and antibacterial, as previously analyzed in patients with respiratory disease (24). As suggested by CD11b up-regulation by AMs following CY treatment in the current mouse model, cytotoxic chemotherapy may also play a role in activation of resident macrophages, and possibly in emergence of ViMs in vaccine-primed lungs. Correlating the human and mouse flow cytometry data or transcriptome data could serve as a means to identify activated lung macrophages important for host defense under a variety of pathological insults.

In conclusion, we demonstrate that exogenous conditioning of the lung microenvironment can expand chemotherapy-stable lung macrophage subsets and protect the chemotherapy-treated host from lethal bacterial infection in the setting of profound bone marrow suppression. This approach may become a framework for new strategies against infectious diseases in the immunocompromised hosts. Finally, we note that medical advances such as systemic chemotherapy, broad radiotherapy, and transplantation were invented recently in the evolutionary history of humans; there is no obvious precedent for these procedures in terms of "natural" adaptation of cells and tissues. Therefore, we conclude that the body has a repertoire of pathways that adapt to broad

tissue damage, and the presence of ViMs in the lungs may be one adaptive pathway selected for other host tissue defense purposes.

Materials and Methods

Bacteria. *P. aeruginosa* strain PAO1Δ*aroA* (*aroA* deletion mutant of strain PAO1; LPS smooth, serogroup O2/O5) was used for vaccination (11). PAO1Δ*aroA* is an auxotrophic mutant that is highly attenuated, as evidenced by clearance from the lung of normal mice within 100 h (11) and also by inability of systemic dissemination even in neutropenic mice (36). *P. aeruginosa* strain IT4 (LPS smooth, serogroup O1, heterologous to the vaccine strain) (10), a clinical blood isolate, was used for i.n. challenge. Bacterial preparation and quantitation were as previously described (13).

Mouse Model. C57BL/6 wild-type mice, *Ccr2*$^{-/-}$ mice, B-cell–deficient (μMT) mice, and *Rag2*$^{-/-}$ mice (all C57BL/6 background) were purchased from The Jackson Laboratory. *Ccr2*$^{-/-}$ mice and *Rag2*$^{-/-}$ mice were bred in-house under specific pathogen-free conditions. Age- and gender-matched mice were used in each experiment. Mice were used according to protocols approved by the Institutional Animal Care and Use Committee of St. Jude Children's Research Hospital. A previously described mouse model was used for immunization and infection during chemotherapy-induced neutropenia (37). Briefly, mice at 6–8 wk of age were anesthetized by i.p. ketamine and xylazine for i.n. inoculation of the live-attenuated vaccine three times at weekly intervals using escalating doses of 1×10^8, 5×10^8, and 1×10^9 cfu. From 67–100% of the bacterial inoculum is consistently and rapidly translocated to the lungs from the nose (38). During the fourth week after vaccination, CY (Sigma–Aldrich) was administered i.p. once daily every other day for 3 d (150 mg/kg per dose) to induce profound neutropenia [absolute neutrophil count (ANC) <50 cells per microliter of blood] from 1 d after the final dose of CY until at least 4 d later (9). During CY treatment, mice were kept on drinking water containing 150 μg/mL gentamicin (Research Product International) to suppress gram-negative bacteria in the gastrointestinal tract (9, 37). In survival experiments, at 4 wk (±2 d) after the final dose of vaccination and 1 d after the final dose of CY, mice were anesthetized by i.p. ketamine and xylazine and challenged i.n. with wild-type *P. aeruginosa* strain IT4 (60–70 cfu as a target dose). Survival was monitored for 10 d after challenge. Age- and gender-matched mice were used for the unimmunized control group. For some experiments, to eliminate macrophages in the airway, clodronate-containing liposomes (39) were administered i.n. to anesthetized mice starting 24 h before bacterial challenge (100 μL per mouse in two divided doses) (9). Liposomes containing PBS were given i.n. to control mice. For histopathology analysis and immunohistochemistry staining, lungs were harvested from euthanized mice and processed as described in *SI Materials and Methods*.

Adoptive Transfer. Macrophages were isolated by flow cytometry from collagenase-digested lungs pooled from immunized plus CY-treated mice at 4 wk after the final dose of vaccination and 2 d after the final dose of CY. Unimmunized mice (12- to 13-wk-old female mice) that had been pretreated with three doses of CY were anesthetized with isoflurane, and administered 1×10^5 live cells of macrophages (in 50 μL of PBS) to the lungs through an endotracheal catheter that was placed by visualization of the larynx (40). Recipient mice were challenged i.n. with *P. aeruginosa* strain IT4 14 h after transfer.

Isolation and Quantitation of Immune Cells from Mice. Lung immune cells from immunized mice were isolated at 4 wk (±2 d) after the third dose of vaccination and 2 d after the third dose of CY unless otherwise specified. BALF was obtained from euthanized mice by injecting and removing 1 mL of ice-cold calcium- and magnesium-free HBSS through exposed trachea three times. For whole-lung cell analysis or cell sorting, lungs were harvested from unchallenged mice and digested with collagenase as described in *SI Materials and Methods*. The absolute number of each cell population in individual mice was calculated by the fraction of the cell population in a sample multiplied by total live cell counts in the same sample. Blood samples were obtained by cardiac puncture in euthanized mice and the ANC was measured by an automated complete blood cell count analyzer with manual differential count on blood smears.

Flow Cytometry and Cell Sorting. After red blood cell lysis, BALF or collagenase-digested lung samples were incubated with anti-CD16/32 antibody (BioLegend) for 20 min on ice and then stained with mAbs (*SI Materials and Methods*). Ly6G^{hi} populations and CD4$^+$, CD8$^+$, or CD19$^+$ populations were out-gated from CD45$^+$ populations and then further analyzed with the gating strategies shown in Fig. S1 (BALF samples), Fig. 3*A* (whole lung), or Fig. S10 (cell sorting).

Gene Expression Analysis. Macrophages were sorted by flow cytometry from collagenase-digested lungs of untreated mice, immunized mice, or immunized plus CY-treated mice at 4 wk after the final dose of vaccination and 2 d after the final dose of CY without bacterial challenge. Five mice from each treatment group were pooled and treated as a single sample to guarantee a large enough number of cells for each assay. Each treatment group consisted of biologically independent triplicates that were processed in three independent experiments. RNA was extracted from the samples using an RNeasy Plus Mini Kit (Qiagen), and the microarray assay was performed using GeneChip Mouse Gene 2.0 ST arrays (Affymetrix) as described in *SI Materials and Methods*.

Cell Cycle Analysis. Mice received i.p. BrdU (Sigma–Aldrich) once daily for three consecutive days (200 mg/kg per dose), and lungs were harvested from the euthanized mice 1 d after the final dose of BrdU (41). Collagenase-digested lung cells were stained for surface markers first and then for intranuclear BrdU using a BrdU Flow Kit (BD Biosciences). Ki-67 staining of lung cells was performed using the same kit with substitution of anti–BrdU-APC Ab with anti–Ki-67-APC Ab (Biolegend) (42). Cells were analyzed by flow cytometry for quantification of BrdU$^+$ or Ki-67$^+$ fractions in macrophage gates.

Phagocytosis Assay. Macrophages were isolated by flow cytometry from collagenase-digested lungs pooled from immunized plus CY-treated mice at 4 wk after the final dose of vaccination and 2 d after the final dose of CY. Cells were incubated in vitro with fluorescent latex beads (43) or CypHer5E-labeled *P. aeruginosa* strain IT4 (32) for 60 min, and then analyzed by flow cytometry for quantification of the fluorescence-positive fractions. For *P. aeruginosa* phagocytosis, cells were supplemented with either intact or heat-inactivated mouse sera obtained from PAO1Δ*aroA*-immunized mice. Cells treated with Cytochalasin D (Sigma–Aldrich) were used for negative controls (44). Further details are provided in *SI Materials and Methods*.

Statistics. Nonparametric data were compared by the Mann–Whitney test for pairwise comparisons or by the Kruskal–Wallis test with Dunn's posttest for comparisons of more than two groups. Parametric data between two groups were compared by unpaired *t* test. Survival curves were compared by log-rank test. *P* values of <0.05 were considered as statistically significant. All of the above analyses were performed using GraphPad Prism software. Statistics used in hierarchical clustering of gene expression data are described in *SI Materials and Methods*.

ACKNOWLEDGMENTS. We thank Drs. Jon McCullers, Terrence Geiger, and Joshua Wolf for discussion; Dr. Richard Ashmun for flow cytometry cell sorting; Dr. Nico van Rooijen for provision of liposomal PBS and clodronate; Mr. Jay Morris and Ms. Melanie Loyd for gene expression assay; and Ms. Meifen Lu for immunohistochemistry staining. This work was supported by a Pediatric Infectious Diseases Society-St. Jude Basic Research Fellowship Grant (to A.K.), Department of Health and Human Services Contract HHSN272201400006C (to P.G.T.), National Institute of Allergy and Infectious Diseases Grant R01AI027913 (to E.I.T.), National Cancer Institute Cancer Center Support Grant P30 CA21765, and the American Lebanese Syrian Associated Charities.

1. Joensuu H (2008) Systemic chemotherapy for cancer: From weapon to treatment. *Lancet Oncol* 9(3):304.
2. Christopher MJ, Link DC (2007) Regulation of neutrophil homeostasis. *Curr Opin Hematol* 14(1):3–8.
3. Freifeld AG, et al.; Infectious Diseases Society of America (2011) Clinical practice guideline for the use of antimicrobial agents in neutropenic patients with cancer: 2010 update by the infectious diseases society of america. *Clin Infect Dis* 52(4):e56–e93.
4. Bodey GP, Buckley M, Sathe YS, Freireich EJ (1966) Quantitative relationships between circulating leukocytes and infection in patients with acute leukemia. *Ann Intern Med* 64(2):328–340.
5. Rosenberg PS, et al.; Severe Chronic Neutropenia International Registry (2006) The incidence of leukemia and mortality from sepsis in patients with severe congenital neutropenia receiving long-term G-CSF therapy. *Blood* 107(12): 4628–4635.
6. Mehta HM, Malandra M, Corey SJ (2015) G-CSF and GM-CSF in neutropenia. *J Immunol* 195(4):1341–1349.
7. Vento S, Cainelli F, Temesgen Z (2008) Lung infections after cancer chemotherapy. *Lancet Oncol* 9(10):982–992.
8. Sun L, et al. (2009) Effect of IL-10 on neutrophil recruitment and survival after Pseudomonas aeruginosa challenge. *Am J Respir Cell Mol Biol* 41(1):76–84.

9. Koh AY, Priebe GP, Ray C, Van Rooijen N, Pier GB (2009) Inescapable need for neutrophils as mediators of cellular innate immunity to acute Pseudomonas aeruginosa pneumonia. *Infect Immun* 77(12):5300–5310.
10. Priebe GP, Meluleni GJ, Coleman FT, Goldberg JB, Pier GB (2003) Protection against fatal Pseudomonas aeruginosa pneumonia in mice after nasal immunization with a live, attenuated aroA deletion mutant. *Infect Immun* 71(3):1453–1461.
11. Priebe GP, et al. (2002) Construction and characterization of a live, attenuated aroA deletion mutant of Pseudomonas aeruginosa as a candidate intranasal vaccine. *Infect Immun* 70(3):1507–1517.
12. Priebe GP, et al. (2008) IL-17 is a critical component of vaccine-induced protection against lung infection by lipopolysaccharide-heterologous strains of Pseudomonas aeruginosa. *J Immunol* 181(7):4965–4975.
13. Kamei A, Coutinho-Sledge YS, Goldberg JB, Priebe GP, Pier GB (2011) Mucosal vaccination with a multivalent, live-attenuated vaccine induces multifactorial immunity against Pseudomonas aeruginosa acute lung infection. *Infect Immun* 79(3):1289–1299.
14. Serbina NV, Hohl TM, Cherny M, Pamer EG (2009) Selective expansion of the monocytic lineage directed by bacterial infection. *J Immunol* 183(3):1900–1910.
15. Samstein M, et al. (2013) Essential yet limited role for CCR2$^+$ inflammatory monocytes during Mycobacterium tuberculosis-specific T cell priming. *eLife* 2:e01086.
16. Xiong H, et al. (2015) Distinct contributions of neutrophils and CCR2+ monocytes to pulmonary clearance of different Klebsiella pneumoniae strains. *Infect Immun* 83(9): 3418–3427.
17. Epelman S, Lavine KJ, Randolph GJ (2014) Origin and functions of tissue macrophages. *Immunity* 41(1):21–35.
18. Guilliams M, et al. (2013) Alveolar macrophages develop from fetal monocytes that differentiate into long-lived cells in the first week of life via GM-CSF. *J Exp Med* 210(10):1977–1992.
19. Lavin Y, Mortha A, Rahman A, Merad M (2015) Regulation of macrophage development and function in peripheral tissues. *Nat Rev Immunol* 15(12):731–744.
20. Ginhoux F, Guilliams M (2016) Tissue-resident macrophage ontogeny and homeostasis. *Immunity* 44(3):439–449.
21. Hashimoto D, et al. (2013) Tissue-resident macrophages self-maintain locally throughout adult life with minimal contribution from circulating monocytes. *Immunity* 38(4): 792–804.
22. Gibbings SL, et al. (2015) Transcriptome analysis highlights the conserved difference between embryonic and postnatal-derived alveolar macrophages. *Blood* 126(11): 1357–1366.
23. Duan M, et al. (2012) Distinct macrophage subpopulations characterize acute infection and chronic inflammatory lung disease. *J Immunol* 189(2):946–955.
24. Duan M, et al. (2016) CD11b immunophenotyping identifies inflammatory profiles in the mouse and human lungs. *Mucosal Immunol* 9(2):550–563*ol*.
25. Gautier EL, et al.; Immunological Genome Consortium (2012) Gene-expression profiles and transcriptional regulatory pathways that underlie the identity and diversity of mouse tissue macrophages. *Nat Immunol* 13(11):1118–1128.
26. Misharin AV, Morales-Nebreda L, Mutlu GM, Budinger GR, Perlman H (2013) Flow cytometric analysis of macrophages and dendritic cell subsets in the mouse lung. *Am J Respir Cell Mol Biol* 49(4):503–510.
27. Zaynagetdinov R, et al. (2013) Identification of myeloid cell subsets in murine lungs using flow cytometry. *Am J Respir Cell Mol Biol* 49(2):180–189.
28. Jakubzick C, et al. (2013) Minimal differentiation of classical monocytes as they survey steady-state tissues and transport antigen to lymph nodes. *Immunity* 39(3):599–610.
29. Kopf M, Schneider C, Nobs SP (2015) The development and function of lung-resident macrophages and dendritic cells. *Nat Immunol* 16(1):36–44.
30. Price JG, et al. (2015) CDKN1A regulates Langerhans cell survival and promotes Treg cell generation upon exposure to ionizing irradiation. *Nat Immunol* 16(10): 1060–1068.
31. Perdiguero EG, Geissmann F (2016) The development and maintenance of resident macrophages. *Nat Immunol* 17(1):2–8.
32. Beletskii A, et al. (2005) High-throughput phagocytosis assay utilizing a pH-sensitive fluorescent dye. *Biotechniques* 39(6):894–897.
33. van de Laar L, et al. (2016) Yolk sac macrophages, fetal liver, and adult monocytes can colonize an empty niche and develop into functional tissue-resident macrophages. *Immunity* 44(4):755–768.
34. Lavin Y, et al. (2014) Tissue-resident macrophage enhancer landscapes are shaped by the local microenvironment. *Cell* 159(6):1312–1326.
35. Westphalen K, et al. (2014) Sessile alveolar macrophages communicate with alveolar epithelium to modulate immunity. *Nature* 506(7489):503–506.
36. Koh AY, Priebe GP, Pier GB (2005) Virulence of Pseudomonas aeruginosa in a murine model of gastrointestinal colonization and dissemination in neutropenia. *Infect Immun* 73(4):2262–2272.
37. Kamei A, et al. (2013) Collaboration between macrophages and vaccine-induced CD4+ T cells confers protection against lethal Pseudomonas aeruginosa pneumonia during neutropenia. *J Infect Dis* 207(1):39–49.
38. Allewelt M, Coleman FT, Grout M, Priebe GP, Pier GB (2000) Acquisition of expression of the Pseudomonas aeruginosa ExoU cytotoxin leads to increased bacterial virulence in a murine model of acute pneumonia and systemic spread. *Infect Immun* 68(7): 3998–4004.
39. Van Rooijen N, Sanders A (1994) Liposome mediated depletion of macrophages: Mechanism of action, preparation of liposomes and applications. *J Immunol Methods* 174(1-2):83–93.
40. Happle C, et al. (2014) Pulmonary transplantation of macrophage progenitors as effective and long-lasting therapy for hereditary pulmonary alveolar proteinosis. *Sci Transl Med* 6(250):250ra113.
41. Balu DT, et al. (2009) Flow cytometric analysis of BrdU incorporation as a high-throughput method for measuring adult neurogenesis in the mouse. *J Pharmacol Toxicol Methods* 59(2):100–107.
42. Challen GA, Boles NC, Chambers SM, Goodell MA (2010) Distinct hematopoietic stem cell subtypes are differentially regulated by TGF-beta1. *Cell Stem Cell* 6(3):265–278.
43. Steinkamp JA, Wilson JS, Saunders GC, Stewart CC (1982) Phagocytosis: Flow cytometric quantitation with fluorescent microspheres. *Science* 215(4528):64–66.
44. DeLoid GM, Sulahian TH, Imrich A, Kobzik L (2009) Heterogeneity in macrophage phagocytosis of Staphylococcus aureus strains: High-throughput scanning cytometry-based analysis. *PLoS One* 4(7):e6209.
45. Irizarry RA, et al. (2003) Exploration, normalization, and summaries of high density oligonucleotide array probe level data. *Biostatistics* 4(2):249–264.